

Chapter 6

FPC Window Mesh Effect and its Correction

Ping Zhao

6.1 Introduction

During the HRMA calibration, the HXDA Flow Proportional Counters (FPC) were filled with P10 gas (90% Ar + 10% CH₄) with a constant pressure of 400 torr and operating temperature of approximately 20°C. The FPC windows were made of 1 μm polyimide (C₂₂H₁₀O₄N₂) with 0.02 μm aluminum coating. A wire mesh was used to support this very thin window membrane under vacuum. The wires were made of 0.1 mm diameter gold-plated tungsten with 2 mm pitch.

As the wires are opaque within the energy range of the calibration X-rays, the mesh changes the FPC window transmission. For BND counters, assuming a uniform distribution of the X-rays, the transmission is decreased by a factor of

$$\frac{(2mm - 0.1mm)^2}{(2mm)^2} = 0.9025 \quad (6.1)$$

(see also §3.2.2). For the focal plane FPC, the transmission decrease due to the mesh is much more complicated. During the VETA-I calibration, the FPC mesh was made with 50.8 μm diameter wire, an average pitch of 529.17 μm, and located 25 mm behind the focal plane. The X-ray transmission varied from 75% to 92%, depending on the phase of the mesh grid relative to the single photon ring on the mesh. (Zhao et al., 1992)

For the HRMA calibration, improvements have been made to reduce the mesh effect: the mesh pitch was increased to 2 mm and the distance between the aperture plate and center of the mesh window was reduced to 9.1±0.2 mm.¹ Thus the four photon rings from the four HRMA shells should be inside one mesh grid cell if the mesh is well centered. The mesh wires should not block any of the focused photons. However, in case the mesh were not centered, its effect can be very severe. Theoretically, it can decrease the transmission by more than 40% in some cases (e.g. when mesh wire block X-rays from one side of the ring 6). Even the mesh were well centered, the mesh wires could still block scattered photons. Therefore, the mesh effect needs to be carefully evaluated and its corrections needs to be calculated in order to obtain the correct calibration results.

This Chapter discusses the mesh effect and its corrections for the on-axis encircled energy measurements.

¹During the calibration, this was thought to be 9.7 mm based on the then available data. It was remeasured after the calibration to be 9.1±0.2 mm.

6.2 HRMA Image on FPC Mesh

Since the FPC mesh window is located about 9.1 mm behind the aperture plate, when the aperture plate was positioned in the HRMA focal plane, the focused X-rays diverge behind the aperture and form four ring patterns entering the mesh window. The diameters of the four rings are 1.06 mm, 0.85 mm, 0.75 mm, and 0.56 mm, respectively. X-rays that fall on the mesh wire will not enter the FPC and therefore will not be counted. (For high energy X-ray photons hit the edge of the wire, some of them may go through. But this effect is very small and completely negligible for our data analysis.)

Figure 6.1 is a HSI image with −9.7 mm defocus with an Al-Kα source. (This was thought to be the FPC mesh position during the calibration. The actual mesh position was measured after the calibration to be −9.1±0.2 mm defocus.) The horizontal line underneath the figure indicates 1 mm. Four rings are clearly shown in the image, as well as the effect due to the gravity and epoxy strain (see Chapter 18). Ring 6 is tilted to the lower left as is known.

6.3 Mesh Transmission Model

Raytracing simulations were made to model the mesh transmission. Figures 6.2–6.5 are simulated images of four individual shells at the mesh window plane (−9.1 mm defocus), with an Al-Kα source. Each figure is 2×2 mm² – the size of a mesh grid cell. For shell 1 the mesh cell has to be centered within 300 μm laterally with respect to the focus in order to avoid the mesh wire. For other shells, this tolerance is larger as the rings are smaller. Figures 6.6–6.9 are simulated images of the full HRMA with four different energies when they enter the mesh window.

The mesh transmission can be modeled by moving a blocking mesh grid with respect to the photon images generated by raytrace. Here the transmission is the ratio of with mesh in place versus without mesh.

Figures 6.10–6.13 show the mesh transmission as a function of Y and Z offset for four individual shells with an Al-Kα source. The plateau in the center of each figure indicates where the mesh is centered well enough so that the transmission is near 100%. For shell 1, the transmission plateau is the smallest because its tolerance is the smallest as mentioned above. For other shells, the plateau becomes larger as their tolerance increases.

Figures 6.14–6.25 show the mesh transmission as a function of Y and Z offset for the full HRMA with four different energies (1.49 keV, 4.51 keV, 6.40 keV, and 8.64 keV) and three aperture sizes (0.01 mm, 1 mm, and 35 mm). The center transmission plateau is smaller for lower energies as most of the X-rays are reflected by shell 1. For higher energies, as less X-rays reflected from outer shells and more X-rays reflected from inner shells, the tolerance of mesh centering becomes larger and so is the plateau. For the 0.01 mm aperture, the transmission plateau is not a square because the aperture cuts off some of the focused photons.

6.4 Mesh Scan

In order to check the exact location of the FPC window mesh with respect to the focus, mesh scan tests were needed in which an aperture was fixed at the focus while the FPC counter scans behind the aperture. During the calibration, three such mesh scans were made. With the 1 mm aperture fixed, FPC-X2 counter (the focal plane FPC detector) were scanned in both Y and Z directions to measure the variations in the counting rate. The scans went from −1.2 mm to 1.2 mm with respect to the current counter location. Table 6.1 lists these three mesh scans.

Table 6.1: HXDS FPC-X2 Mesh Scans

Date (GMT)	Run ID	TRW ID	Source	Aperture	Y-offset	Z-offset
961221	106785	C-IXF-FM-3.001	Al-K α	1.0 mm	-0.4176 mm	-0.0827 mm
961224	106926	C-IXF-FM-61.001	Al-K α	1.0 mm	-0.3978 mm	-0.0221 mm
970115	108922	D-IXF-FM-3.002	C-K α	1.0 mm	+0.0188 mm	-0.1449 mm

By fitting the mesh scan data to the mesh transmission model, the exact mesh positions can be located. Figures 6.26–6.28 show these three pairs of mesh scan data and their fit to the mesh transmission model. It is obvious that the first two scans reveal the mesh was offset in the Y direction by about 400 μm .

After the first mesh scan was made on 1996/12/21, it was known that the mesh center was off. But no corrections were made as that was at the very beginning of the calibration. Three days later, after the second mesh scan was made, a correction was made to bring the mesh center aligned with the aperture center, using a quick look analysis. When the third mesh scans were made on 1997/01/15, the mesh was still reasonably well centered. According to the scan data, it was only off very little in the Z-axis. This could be due to the counter was drifting off slowly, or the original centering was not perfect. On 1997/01/16, a mesh center correction of +95 μm in the Z-direction was made based on a quick look analysis of mesh scan data on 1997/01/15.

Therefore, there were four mesh center positions during the calibration, based on the mesh scan data and subsequent corrections. Table 6.2 lists these mesh positions. We do not know the exact location between the mesh scan measurements. It might have drifted a little, but that should not be too much. Figure 6.29 shows these mesh center positions during the calibration.

Table 6.2: HXDS FPC-X2 Mesh Center Positions

Position	Dates (GMT)	Run IDs	Y-offset	Z-offset
1	1996/12/20 – 1996/12/21	106697 – 106785	-0.4176 mm	-0.0827 mm
2	1996/12/21 – 1996/12/24	106786 – 106926	-0.3978 mm	-0.0221 mm
3	1996/12/24 – 1997/01/16	106927 – 109015	+0.0188 mm	-0.1449 mm
4	1997/01/16 – 1997/02/11	109016 – 111906	+0.0188 mm	-0.0499 mm

As all the HRMA on-axis encircled energy measurements were made during the phase D and E of the calibration, i.e. period of 1996/12/31 – 1997/02/11, only mesh position 3 and 4 are relevant for calculating the mesh effect corrections.

6.5 Mesh Correction

Using the mesh center offset at positions 3 and 4, the mesh transmission can be calculated using the raytrace simulation. Mesh correction is the reciprocal of the calculated mesh transmission.

Tables 6.3 – 6.7 give the mesh effect correction factors for Shell 1, Shell 3, Shell 4, Shell 6, and HRMA, respectively. Aperture diameters and the X-ray energies are the ones actually used for the calibration. At the inter section of Aperture and Energy, the Tables give the corresponding mesh correction factor. For example, for Shell 1, Zn-K source (8.6389 keV), 35 mm aperture, and

on 1997/01/20, the on-axis FPC encircled energy result needs a mesh correction of 1.0284 (this actually is the largest mesh correction factor in all five tables). Because the HXDS system was properly designed and the mesh was well centered during the encircled energy measurements, the mesh effect was very small. Except for Shell 1 and large aperture, higher energies, most of the correction factors are less than 1%. No corrections are needed for apertures less or equal to 0.5 mm diameter.

6.6 Conclusion

Based on the mesh scan data taken during the HRMA calibration and raytracing simulations, the HXDS FPC window mesh effects were studied and its correction factors were calculated. For the on-axis encircled energy measurements,² the mesh effect was very small. Except for Shell 1 and large aperture, higher energies, most of the correction factors are less than 1%. The mesh effect corrections are listed in five tables at the end of this Chapter.

²For the off-axis encircled energy measurements, the mesh effects are much more severe and complicated (depends on the off-axis angle and direction), which is beyond the scope of this Chapter.

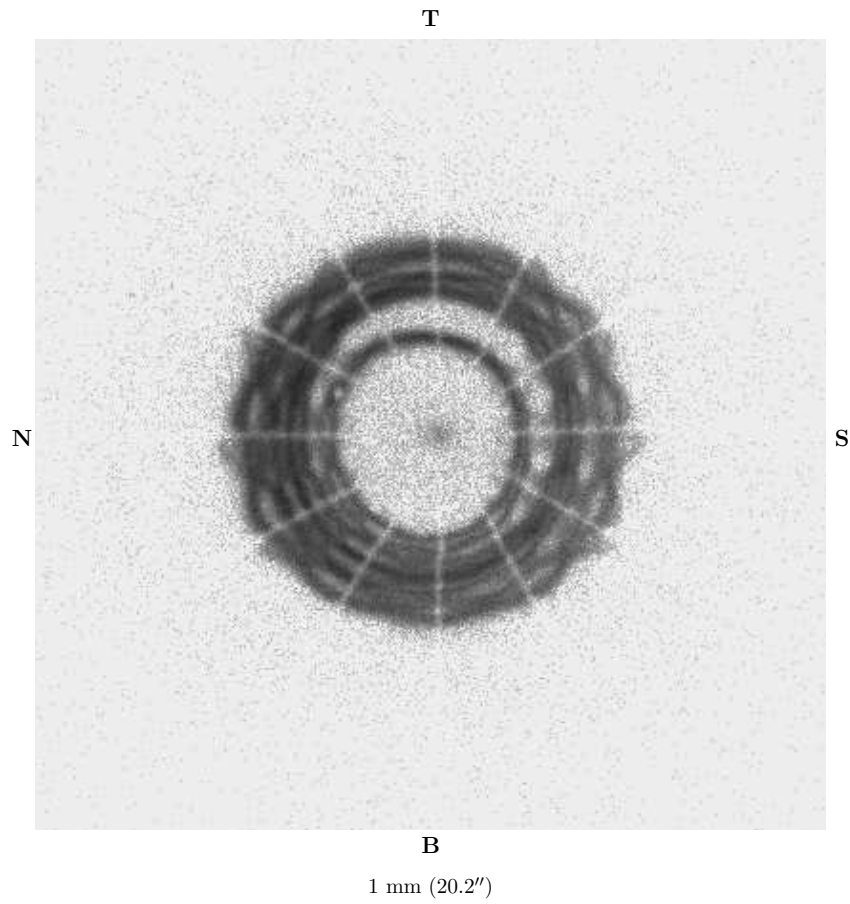


Figure 6.1: The HRMA HSI image with -9.7 mm defocus. (This was thought to be the FPC mesh position during the calibration. The actual mesh position was measured after the calibration to be -9.1 ± 0.2 mm defocus.) Date: 97/01/15; TRW ID: E-IXH-RF-18.002; Run ID: 111803; Source: Al-K α ; Defocus: -9.7 mm; Integration time: 1000 seconds.

Simulated XRCF HRMA Images on FPC Window Mesh
 Four Shells Source: Al-K α (1.49 keV) -9.1 mm Defocus

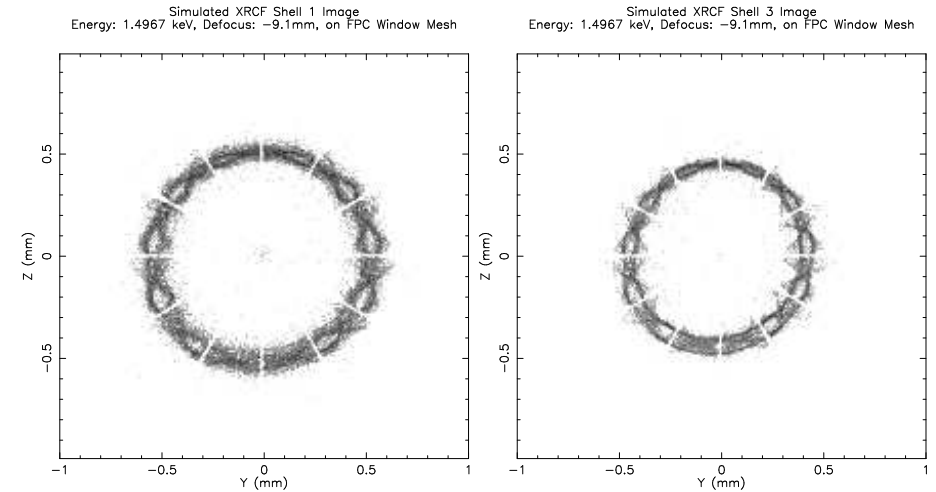


Figure 6.2: Shell 1

Figure 6.3: Shell 3

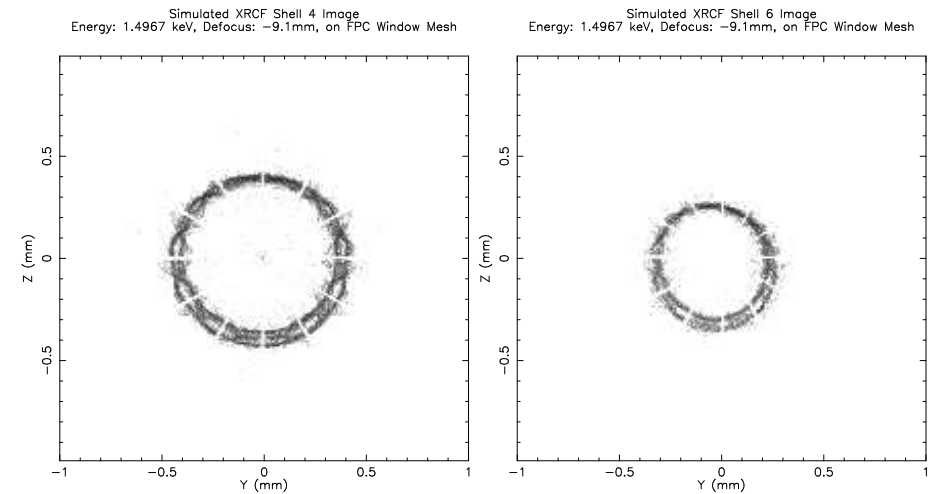


Figure 6.4: Shell 4

Figure 6.5: Shell 6

Simulated XRCF HRMA Images on FPC Window Mesh

Full HRMA Four Energies -9.1 mm Defocus

Simulated XRCF HRMA Image
Energy: 1.4967 keV, Defocus: -9.1mm, on FPC Window Mesh

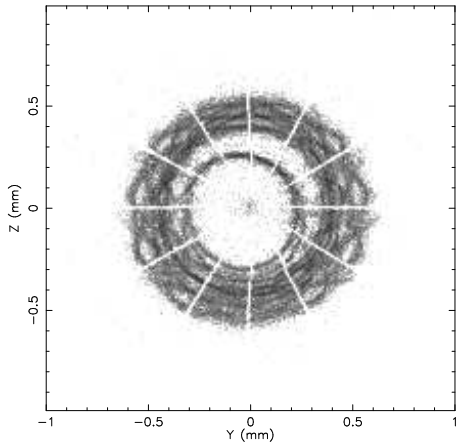


Figure 6.6: Al-K α (1.49 keV)

Simulated XRCF HRMA Image
Energy: 4.51084 keV, Defocus: -9.1mm, on FPC Window Mesh

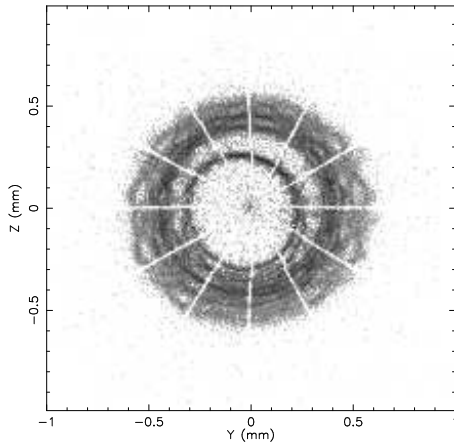


Figure 6.7: Ti-K α (4.51 keV)

Simulated XRCF HRMA Image
Energy: 6.40384 keV, Defocus: -9.1mm, on FPC Window Mesh

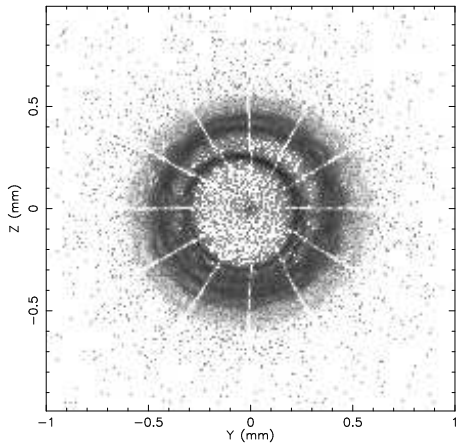


Figure 6.8: Fe-K α (6.40 keV)

Simulated XRCF HRMA Image
Energy: 8.63886 keV, Defocus: -9.1mm, on FPC Window Mesh

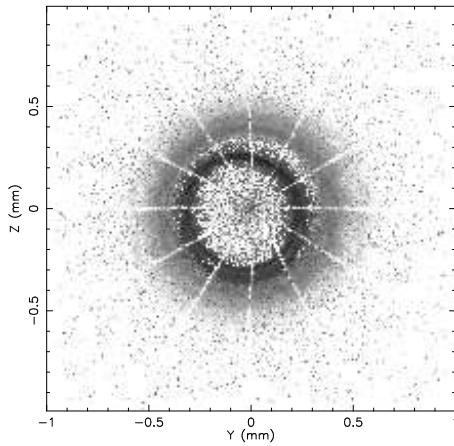


Figure 6.9: Zn-K α (8.64 keV)

Mesh Window Transmission Model

Four Shells Source: Al-K α (1.49 keV) 1.0 mm Aperture

Mesh Window Transmission Model
Shell 1 Energy: 1.496 keV Aperture: 1.000 mm

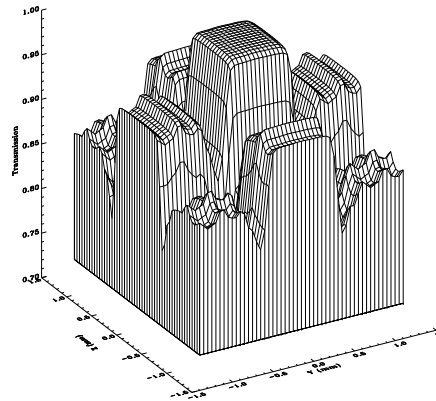


Figure 6.10: Al-K α . Shell 1.

Mesh Window Transmission Model
Shell 3 Energy: 1.496 keV Aperture: 1.000 mm

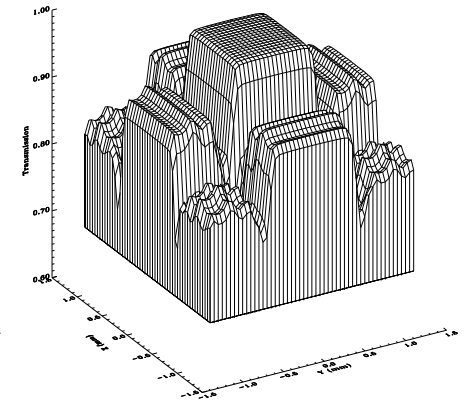


Figure 6.11: Al-K α . Shell 3.

Mesh Window Transmission Model
Shell 4 Energy: 1.496 keV Aperture: 1.000 mm

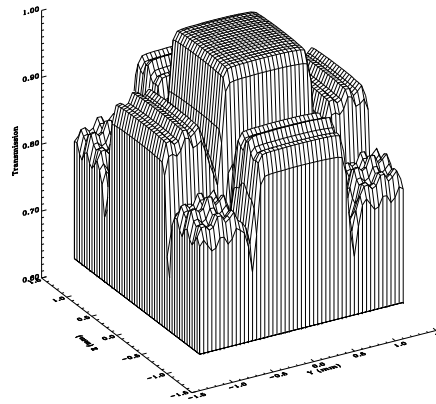


Figure 6.12: Al-K α . Shell 4.

Mesh Window Transmission Model
Shell 6 Energy: 1.496 keV Aperture: 1.000 mm

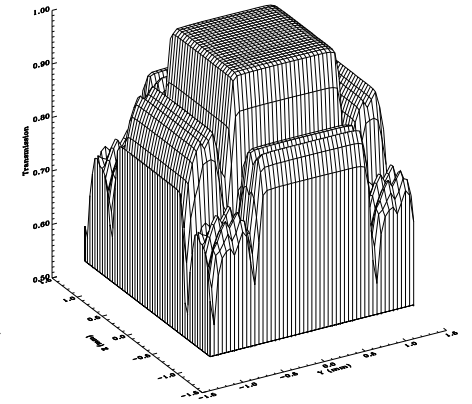
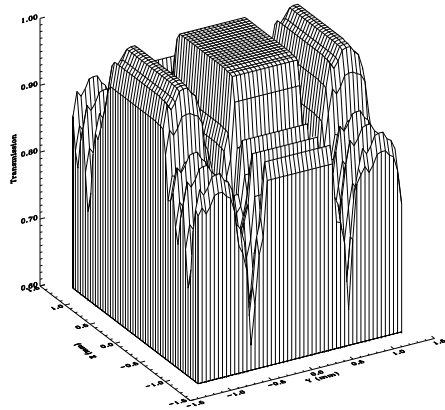


Figure 6.13: Al-K α . Shell 6.

Mesh Window Transmission Model
 Full HRMA Four Energies 0.01 mm Aperture

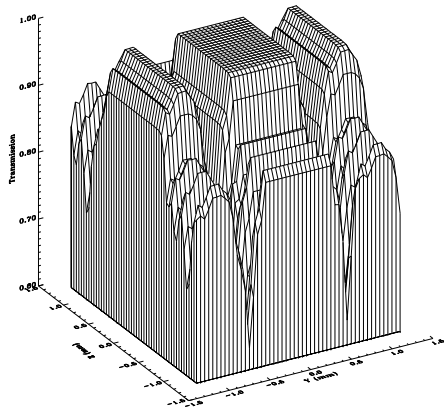
Mesh Window Transmission Model
 HRMA Energy: 1.496 keV Aperture: 0.010 mm



Zhao/SAO 09/08/98 10:40:11

Figure 6.14: Al-K α . HRMA.

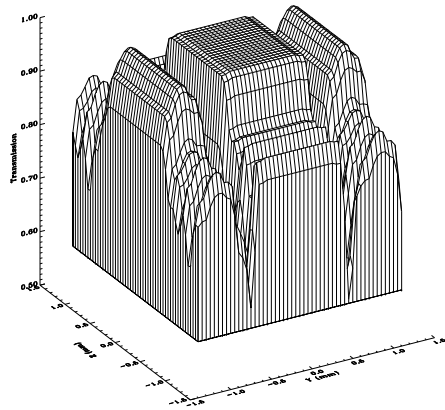
Mesh Window Transmission Model
 HRMA Energy: 4.510 keV Aperture: 0.010 mm



Zhao/SAO 09/08/98 10:40:11

Figure 6.15: Ti-K α . HRMA.

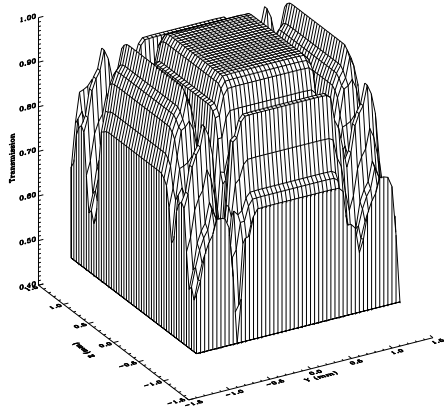
Mesh Window Transmission Model
 HRMA Energy: 6.403 keV Aperture: 0.010 mm



Zhao/SAO 09/08/98 10:40:11

Figure 6.16: Fe-K α . HRMA.

Mesh Window Transmission Model
 HRMA Energy: 8.638 keV Aperture: 0.010 mm

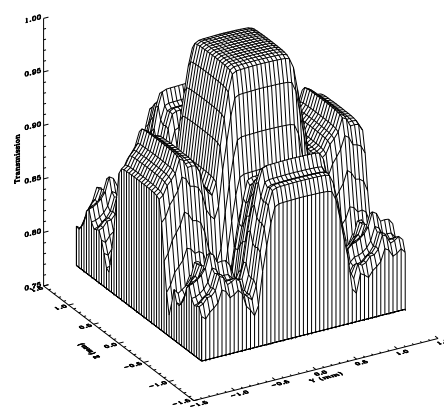


Zhao/SAO 09/08/98 10:40:11

Figure 6.17: Zn-K α . HRMA.

Mesh Window Transmission Model
 Full HRMA Four Energies 1.0 mm Aperture

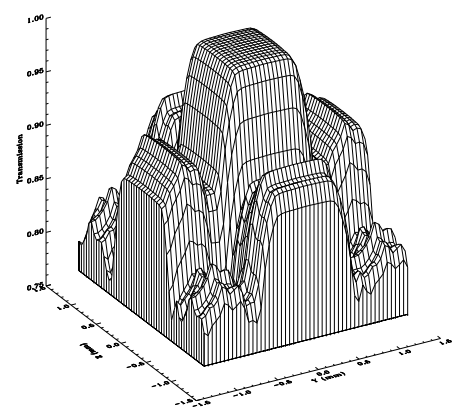
Mesh Window Transmission Model
 HRMA Energy: 1.496 keV Aperture: 1.000 mm



Zhao/SAO 09/08/98 10:40:11

Figure 6.18: Al-K α . HRMA.

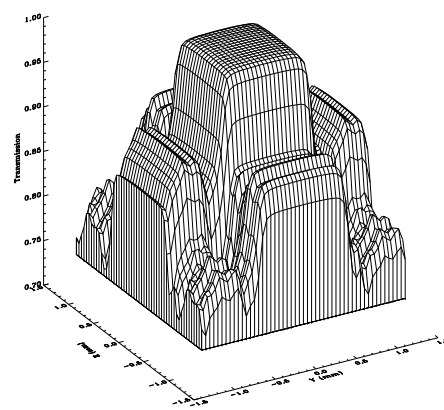
Mesh Window Transmission Model
 HRMA Energy: 4.510 keV Aperture: 1.000 mm



Zhao/SAO 09/08/98 10:40:11

Figure 6.19: Ti-K α . HRMA.

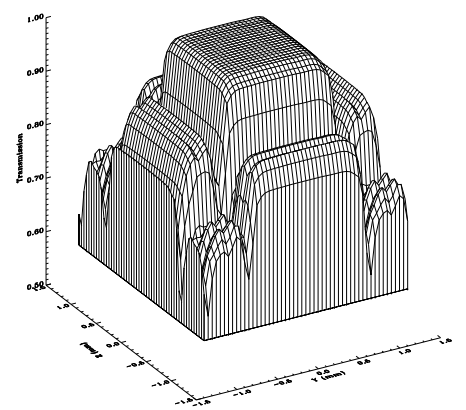
Mesh Window Transmission Model
 HRMA Energy: 6.403 keV Aperture: 1.000 mm



Zhao/SAO 09/08/98 10:40:11

Figure 6.20: Fe-K α . HRMA.

Mesh Window Transmission Model
 HRMA Energy: 8.638 keV Aperture: 1.000 mm

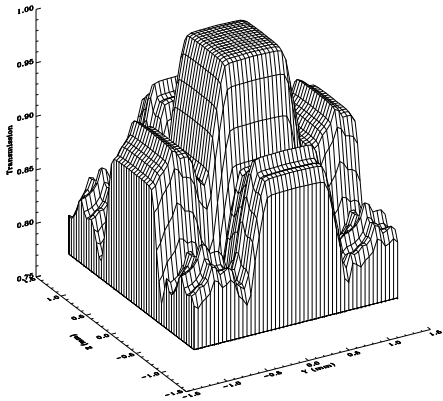


Zhao/SAO 09/08/98 10:40:11

Figure 6.21: Zn-K α . HRMA.

Mesh Window Transmission Model Full HRMA Four Energies 35.0 mm Aperture

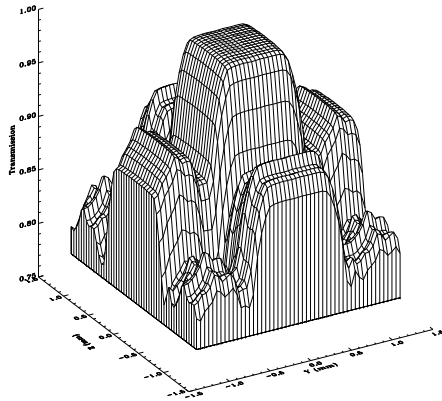
Mesh Window Transmission Model
HRMA Energy: 1.496 keV Aperture: 35.00 mm



Zhao/SAO 09/08/98 10:40:11

Figure 6.22: Al-K α . HRMA.

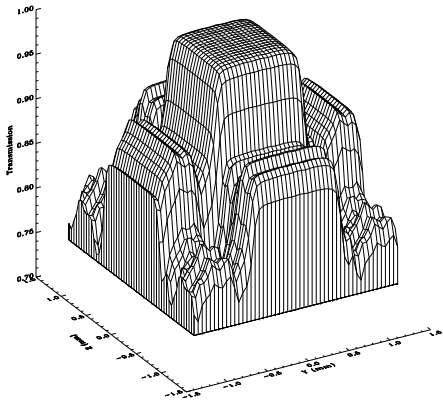
Mesh Window Transmission Model
HRMA Energy: 4.510 keV Aperture: 35.00 mm



Zhao/SAO 09/08/98 10:40:11

Figure 6.23: Ti-K α . HRMA.

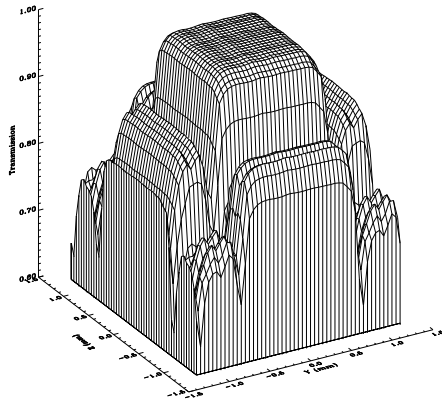
Mesh Window Transmission Model
HRMA Energy: 6.403 keV Aperture: 35.00 mm



Zhao/SAO 09/08/98 10:40:11

Figure 6.24: Fe-K α . HRMA.

Mesh Window Transmission Model
HRMA Energy: 8.638 keV Aperture: 35.00 mm

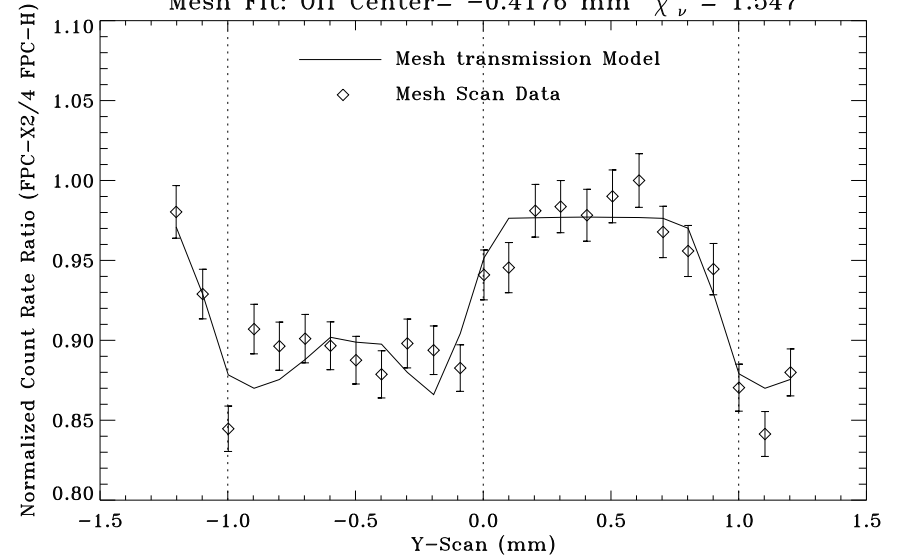


Zhao/SAO 09/08/98 10:40:11

Figure 6.25: Zn-K α . HRMA.

HXDS FPC-X2 Mesh Scan

Mesh Fit: Off Center= -0.4176 mm $\chi^2_\nu = 1.547$



Mesh Fit: Off Center= -0.0827 mm $\chi^2_\nu = 1.018$

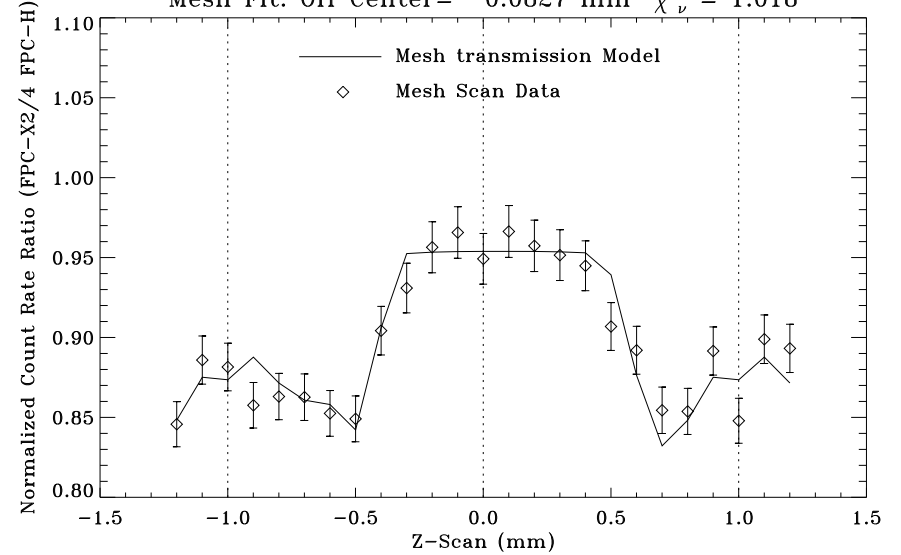


Figure 6.26: HXDS FPC-X2 Mesh Scan data fit to the model. Date: 96/12/21; TRW ID: C-IXF-FM-3.001; Run ID: 106785; Source: Al-K α .

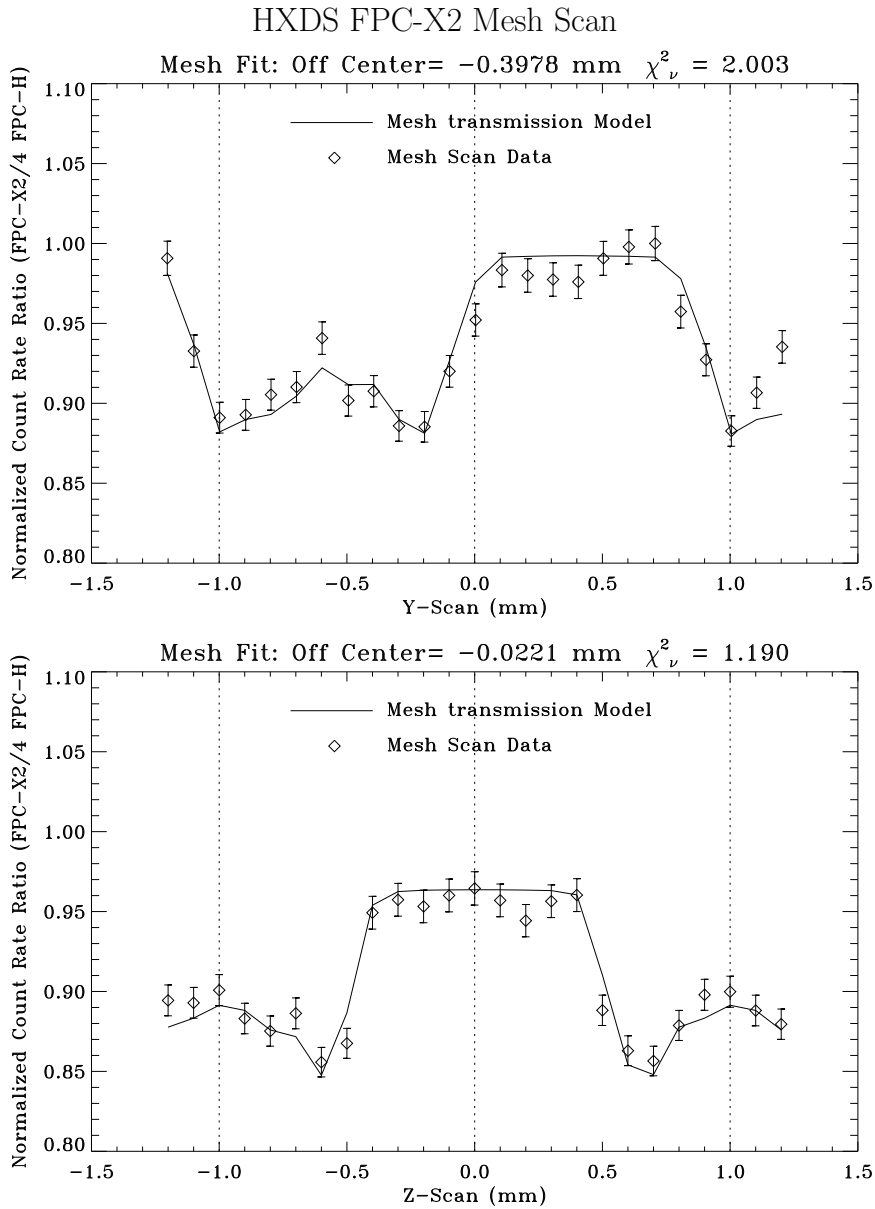


Figure 6.27: HXDS FPC-X2 Mesh Scan data fit to the model. Date: 96/12/24; TRW ID: C-IXF-FM-61.001; Run ID: 106926; Source: Al-K α .

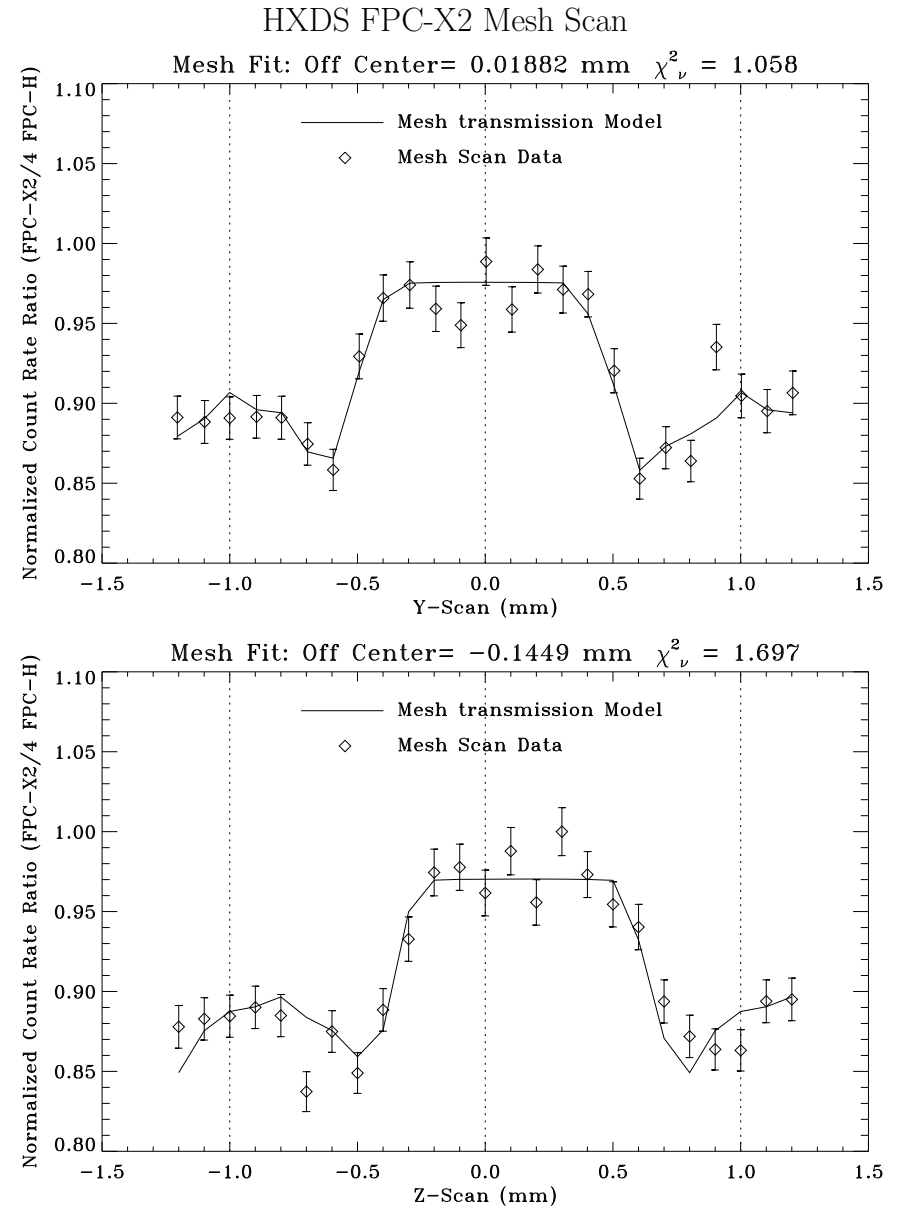


Figure 6.28: HXDS FPC-X2 Mesh Scan data fit to the model. Date: 97/01/15; TRW ID: D-IXF-FM-3.002; Run ID: 108922; Source: C-K α .

HXDS FPC-X2 Mesh Center Offset

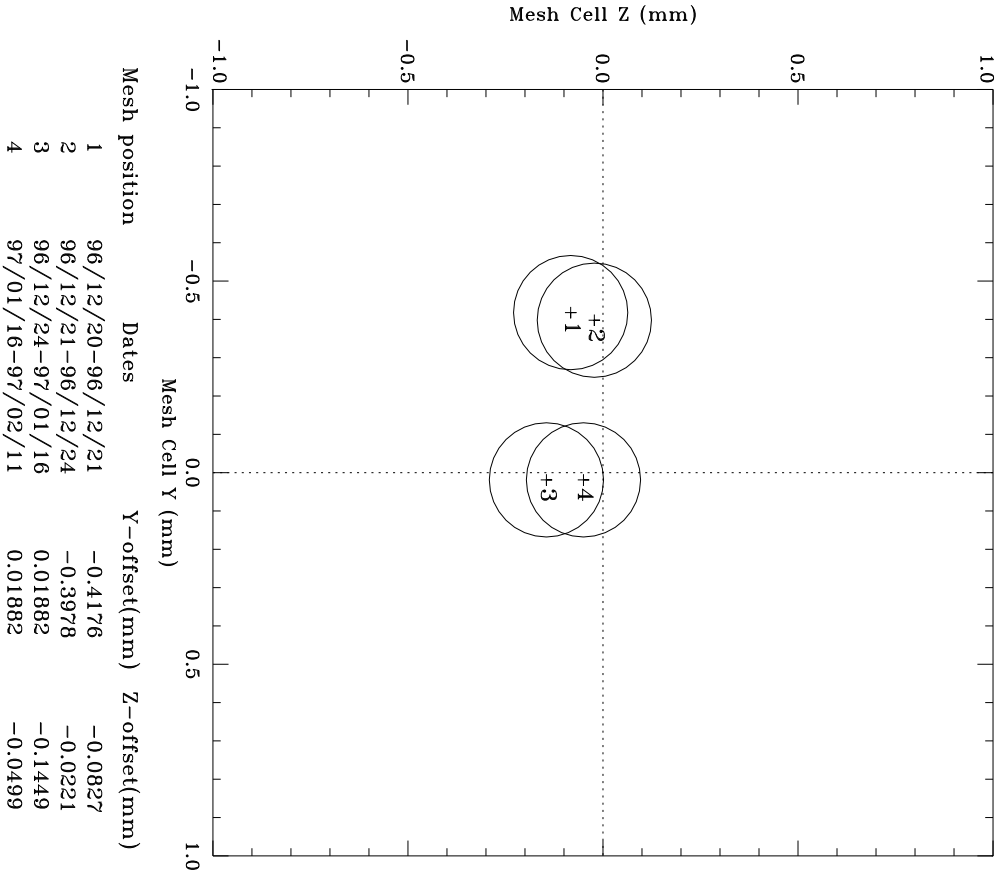


Figure 6.29: HXDS FPC-X2 Mesh Center Offset.

Table 6.3: XRCF HRMA Effective Area Measurements FPC Window Mesh Corrections

Shell 1

Date: 1996/12/24 - 1997/01/16

Mesh offset: Y = 0.0188 mm, Z = -0.1449 mm

Aperture (mm)	Energy (keV)													
	0.1085	0.1833	0.2770	0.5230	0.9297	1.4967	2.0424	2.9843	3.4440	4.5108	5.4147	6.4038	8.0478	8.6389
≤0.50	1.0000	1.0000	1.0000	1.0000	1.0000	1.0000	1.0000	1.0000	1.0000	1.0000	1.0000	1.0000	1.0000	1.0000
1.00	1.0001	1.0001	1.0003	1.0006	1.0007	1.0006	1.0008	1.0008	1.0008	1.0012	1.0016	1.0016	1.0031	1.0031
2.00	1.0001	1.0003	1.0006	1.0010	1.0015	1.0017	1.0017	1.0025	1.0024	1.0033	1.0043	1.0059	1.0103	1.0102
4.00	1.0002	1.0004	1.0008	1.0013	1.0020	1.0021	1.0023	1.0035	1.0038	1.0061	1.0082	1.0108	1.0155	1.0169
10.0	1.0003	1.0005	1.0008	1.0014	1.0024	1.0027	1.0035	1.0050	1.0063	1.0091	1.0119	1.0150	1.0215	1.0229
20.0	1.0003	1.0005	1.0009	1.0016	1.0027	1.0031	1.0041	1.0061	1.0073	1.0105	1.0137	1.0172	1.0246	1.0261
35.0	1.0003	1.0005	1.0009	1.0017	1.0029	1.0033	1.0043	1.0070	1.0080	1.0114	1.0147	1.0191	1.0264	1.0283

Date: 1997/01/16 - 1997/02/11

Mesh offset: Y = 0.0188 mm, Z = -0.0499 mm

Aperture (mm)	Energy (keV)													
	0.1085	0.1833	0.2770	0.5230	0.9297	1.4967	2.0424	2.9843	3.4440	4.5108	5.4147	6.4038	8.0478	8.6389
≤0.50	1.0000	1.0000	1.0000	1.0000	1.0000	1.0000	1.0000	1.0000	1.0000	1.0000	1.0000	1.0000	1.0000	1.0000
1.00	1.0000	1.0002	1.0001	1.0002	1.0006	1.0004	1.0006	1.0005	1.0005	1.0009	1.0017	1.0019	1.0022	1.0028
2.00	1.0001	1.0003	1.0003	1.0008	1.0013	1.0014	1.0016	1.0020	1.0021	1.0028	1.0045	1.0058	1.0090	1.0103
4.00	1.0002	1.0004	1.0005	1.0012	1.0017	1.0020	1.0022	1.0031	1.0037	1.0058	1.0085	1.0101	1.0143	1.0172
10.0	1.0003	1.0005	1.0006	1.0012	1.0023	1.0024	1.0033	1.0052	1.0060	1.0089	1.0122	1.0137	1.0199	1.0232
20.0	1.0003	1.0006	1.0006	1.0013	1.0026	1.0028	1.0038	1.0062	1.0069	1.0103	1.0140	1.0162	1.0229	1.0264
35.0	1.0004	1.0006	1.0006	1.0014	1.0028	1.0030	1.0040	1.0069	1.0077	1.0110	1.0152	1.0175	1.0243	1.0284

Table 6.4: XRCF HRMA Effective Area Measurements FPC Window Mesh Corrections

Shell 3

Date: 1996/12/24 – 1997/01/16

Mesh offset: Y = 0.0188 mm, Z = -0.1449 mm

Aperture (mm)	Energy (keV)													
	0.1085	0.1833	0.2770	0.5230	0.9297	1.4967	2.0424	2.9843	3.4440	4.5108	5.4147	6.4038	8.0478	8.6389
≤0.50	1.0000	1.0000	1.0000	1.0000	1.0000	1.0000	1.0000	1.0000	1.0000	1.0000	1.0000	1.0000	1.0000	1.0000
1.00	1.0000	1.0001	1.0000	1.0003	1.0001	1.0002	1.0001	1.0000	1.0000	1.0001	1.0002	1.0003	1.0006	1.0006
2.00	1.0001	1.0001	1.0002	1.0003	1.0002	1.0004	1.0004	1.0004	1.0008	1.0010	1.0010	1.0012	1.0023	1.0025
4.00	1.0001	1.0001	1.0002	1.0003	1.0003	1.0004	1.0005	1.0005	1.0006	1.0009	1.0016	1.0017	1.0028	1.0046
10.0	1.0001	1.0001	1.0003	1.0003	1.0004	1.0005	1.0005	1.0011	1.0011	1.0026	1.0025	1.0039	1.0057	1.0059
20.0	1.0001	1.0001	1.0003	1.0003	1.0004	1.0005	1.0006	1.0014	1.0014	1.0030	1.0027	1.0045	1.0063	1.0064
35.0	1.0001	1.0001	1.0003	1.0003	1.0004	1.0006	1.0007	1.0014	1.0016	1.0031	1.0029	1.0046	1.0067	1.0069

Date: 1997/01/16 – 1997/02/11

Mesh offset: Y = 0.0188 mm, Z = -0.0499 mm

Aperture (mm)	Energy (keV)													
	0.1085	0.1833	0.2770	0.5230	0.9297	1.4967	2.0424	2.9843	3.4440	4.5108	5.4147	6.4038	8.0478	8.6389
≤0.50	1.0000	1.0000	1.0000	1.0000	1.0000	1.0000	1.0000	1.0000	1.0000	1.0000	1.0000	1.0000	1.0000	1.0000
1.00	1.0000	1.0000	1.0000	1.0000	1.0000	1.0000	1.0000	1.0001	1.0000	1.0000	1.0000	1.0000	1.0000	1.0001
2.00	1.0001	1.0000	1.0001	1.0001	1.0001	1.0002	1.0003	1.0006	1.0007	1.0008	1.0009	1.0010	1.0023	1.0024
4.00	1.0001	1.0000	1.0001	1.0001	1.0003	1.0003	1.0003	1.0007	1.0009	1.0015	1.0019	1.0025	1.0045	1.0046
10.0	1.0001	1.0000	1.0002	1.0002	1.0003	1.0003	1.0004	1.0014	1.0012	1.0024	1.0029	1.0037	1.0056	1.0058
20.0	1.0001	1.0000	1.0002	1.0002	1.0003	1.0003	1.0005	1.0015	1.0014	1.0030	1.0032	1.0043	1.0062	1.0062
35.0	1.0001	1.0000	1.0002	1.0002	1.0003	1.0004	1.0005	1.0015	1.0014	1.0030	1.0035	1.0044	1.0068	1.0069

Table 6.5: XRCF HRMA Effective Area Measurements FPC Window Mesh Corrections

Shell 4

Date: 1996/12/24 – 1997/01/16

Mesh offset: Y = 0.0188 mm, Z = -0.1449 mm

Aperture (mm)	Energy (keV)													
	0.1085	0.1833	0.2770	0.5230	0.9297	1.4967	2.0424	2.9843	3.4440	4.5108	5.4147	6.4038	8.0478	8.6389
≤0.50	1.0000	1.0000	1.0000	1.0000	1.0000	1.0000	1.0000	1.0000	1.0000	1.0000	1.0000	1.0000	1.0000	1.0000
1.00	1.0000	1.0000	1.0001	1.0001	1.0001	1.0000	1.0001	1.0002	1.0000	1.0000	1.0003	1.0004	1.0002	1.0001
2.00	1.0000	1.0001	1.0002	1.0006	1.0004	1.0008	1.0008	1.0008	1.0006	1.0009	1.0010	1.0015	1.0023	1.0029
4.00	1.0000	1.0001	1.0003	1.0009	1.0007	1.0011	1.0016	1.0014	1.0012	1.0017	1.0024	1.0033	1.0051	1.0052
10.0	1.0000	1.0001	1.0004	1.0009	1.0008	1.0012	1.0017	1.0017	1.0019	1.0024	1.0031	1.0042	1.0063	1.0069
20.0	1.0000	1.0001	1.0004	1.0010	1.0008	1.0013	1.0019	1.0020	1.0021	1.0027	1.0033	1.0049	1.0072	1.0075
35.0	1.0000	1.0001	1.0004	1.0010	1.0008	1.0015	1.0020	1.0021	1.0022	1.0029	1.0035	1.0053	1.0077	1.0079

Date: 1997/01/16 – 1997/02/11

Mesh offset: Y = 0.0188 mm, Z = -0.0499 mm

Aperture (mm)	Energy (keV)													
	0.1085	0.1833	0.2770	0.5230	0.9297	1.4967	2.0424	2.9843	3.4440	4.5108	5.4147	6.4038	8.0478	8.6389
≤0.50	1.0000	1.0000	1.0000	1.0000	1.0000	1.0000	1.0000	1.0000	1.0000	1.0000	1.0000	1.0000	1.0000	1.0000
1.00	1.0000	1.0000	1.0000	1.0000	1.0000	1.0000	1.0000	1.0000	1.0000	1.0000	1.0000	1.0000	1.0000	1.0000
2.00	1.0001	1.0001	1.0002	1.0006	1.0004	1.0009	1.0008	1.0007	1.0005	1.0008	1.0012	1.0011	1.0024	1.0030
4.00	1.0001	1.0001	1.0004	1.0008	1.0004	1.0012	1.0012	1.0014	1.0009	1.0018	1.0026	1.0030	1.0044	1.0052
10.0	1.0001	1.0001	1.0004	1.0009	1.0005	1.0013	1.0014	1.0016	1.0017	1.0026	1.0034	1.0039	1.0058	1.0067
20.0	1.0001	1.0001	1.0004	1.0009	1.0006	1.0014	1.0015	1.0018	1.0020	1.0029	1.0039	1.0044	1.0064	1.0080
35.0	1.0001	1.0001	1.0004	1.0009	1.0006	1.0015	1.0016	1.0019	1.0022	1.0031	1.0042	1.0048	1.0068	1.0082

Table 6.6: XRCF HRMA Effective Area Measurements FPC Window Mesh Corrections

Shell 6

Date: 1996/12/24 - 1997/01/16

Mesh offset: Y = 0.0188 mm, Z = -0.1449 mm

Aperture (mm)	Energy (keV)													
	0.1085	0.1833	0.2770	0.5230	0.9297	1.4967	2.0424	2.9843	3.4440	4.5108	5.4147	6.4038	8.0478	8.6389
≤0.50	1.0000	1.0000	1.0000	1.0000	1.0000	1.0000	1.0000	1.0000	1.0000	1.0000	1.0000	1.0000	1.0000	1.0000
1.00	1.0000	1.0000	1.0000	1.0000	1.0000	1.0000	1.0000	1.0000	1.0000	1.0000	1.0000	1.0000	1.0000	1.0000
2.00	1.0001	1.0000	1.0001	1.0004	1.0004	1.0006	1.0009	1.0009	1.0010	1.0010	1.0007	1.0008	1.0013	1.0012
4.00	1.0001	1.0000	1.0001	1.0009	1.0007	1.0008	1.0011	1.0014	1.0018	1.0019	1.0015	1.0018	1.0027	1.0034
10.0	1.0001	1.0004	1.0002	1.0009	1.0009	1.0008	1.0012	1.0018	1.0022	1.0024	1.0026	1.0025	1.0040	1.0052
20.0	1.0001	1.0004	1.0002	1.0009	1.0010	1.0009	1.0013	1.0020	1.0024	1.0026	1.0032	1.0027	1.0046	1.0061
35.0	1.0001	1.0004	1.0002	1.0010	1.0010	1.0009	1.0015	1.0021	1.0024	1.0027	1.0033	1.0032	1.0047	1.0066

Date: 1997/01/16 - 1997/02/11

Mesh offset: Y = 0.0188 mm, Z = -0.0499 mm

Aperture (mm)	Energy (keV)													
	0.1085	0.1833	0.2770	0.5230	0.9297	1.4967	2.0424	2.9843	3.4440	4.5108	5.4147	6.4038	8.0478	8.6389
≤0.50	1.0000	1.0000	1.0000	1.0000	1.0000	1.0000	1.0000	1.0000	1.0000	1.0000	1.0000	1.0000	1.0000	1.0000
1.00	1.0000	1.0000	1.0000	1.0000	1.0000	1.0000	1.0000	1.0000	1.0000	1.0000	1.0000	1.0000	1.0000	1.0000
2.00	1.0000	1.0000	1.0001	1.0001	1.0006	1.0005	1.0008	1.0007	1.0006	1.0009	1.0008	1.0013	1.0011	1.0008
4.00	1.0000	1.0000	1.0001	1.0007	1.0008	1.0008	1.0011	1.0014	1.0016	1.0019	1.0018	1.0021	1.0026	1.0031
10.0	1.0000	1.0004	1.0002	1.0007	1.0010	1.0009	1.0012	1.0016	1.0020	1.0022	1.0029	1.0033	1.0037	1.0048
20.0	1.0000	1.0004	1.0002	1.0007	1.0011	1.0010	1.0013	1.0017	1.0023	1.0024	1.0033	1.0039	1.0041	1.0058
35.0	1.0000	1.0004	1.0002	1.0008	1.0011	1.0010	1.0013	1.0017	1.0023	1.0026	1.0034	1.0043	1.0043	1.0061

Table 6.7: XRCF HRMA Effective Area Measurements FPC Window Mesh Corrections

HRMA

Date: 1996/12/24 - 1997/01/16

Mesh offset: Y = 0.0188 mm, Z = -0.1449 mm

Aperture (mm)	Energy (keV)													
	0.1085	0.1833	0.2770	0.5230	0.9297	1.4967	2.0424	2.9843	3.4440	4.5108	5.4147	6.4038	8.0478	8.6389
≤0.50	1.0000	1.0000	1.0000	1.0000	1.0000	1.0000	1.0000	1.0000	1.0000	1.0000	1.0000	1.0000	1.0000	1.0000
1.00	1.0000	1.0001	1.0002	1.0003	1.0003	1.0003	1.0004	1.0003	1.0003	1.0004	1.0004	1.0003	1.0001	1.0000
2.00	1.0001	1.0002	1.0003	1.0006	1.0008	1.0010	1.0010	1.0012	1.0013	1.0016	1.0014	1.0013	1.0015	1.0014
4.00	1.0001	1.0002	1.0004	1.0009	1.0011	1.0013	1.0015	1.0018	1.0020	1.0029	1.0028	1.0029	1.0032	1.0036
10.0	1.0002	1.0003	1.0005	1.0010	1.0013	1.0015	1.0020	1.0026	1.0031	1.0043	1.0041	1.0038	1.0046	1.0054
20.0	1.0002	1.0003	1.0005	1.0010	1.0015	1.0017	1.0023	1.0032	1.0037	1.0050	1.0046	1.0044	1.0052	1.0062
35.0	1.0002	1.0003	1.0005	1.0011	1.0016	1.0019	1.0024	1.0035	1.0040	1.0054	1.0050	1.0047	1.0054	1.0067

Date: 1997/01/16 - 1997/02/11

Mesh offset: Y = 0.0188 mm, Z = -0.0499 mm

Aperture (mm)	Energy (keV)													
	0.1085	0.1833	0.2770	0.5230	0.9297	1.4967	2.0424	2.9843	3.4440	4.5108	5.4147	6.4038	8.0478	8.6389
≤0.50	1.0000	1.0000	1.0000	1.0000	1.0000	1.0000	1.0000	1.0000	1.0000	1.0000	1.0000	1.0000	1.0000	1.0000
1.00	1.0000	1.0001	1.0001	1.0001	1.0002	1.0002	1.0002	1.0002	1.0002	1.0003	1.0002	1.0000	1.0000	1.0000
2.00	1.0001	1.0002	1.0002	1.0005	1.0007	1.0009	1.0009	1.0011	1.0011	1.0014	1.0015	1.0012	1.0014	1.0009
4.00	1.0001	1.0002	1.0003	1.0007	1.0009	1.0012	1.0013	1.0018	1.0019	1.0028	1.0031	1.0027	1.0030	1.0033
10.0	1.0002	1.0003	1.0004	1.0008	1.0012	1.0014	1.0018	1.0027	1.0030	1.0043	1.0044	1.0039	1.0042	1.0049
20.0	1.0002	1.0003	1.0004	1.0008	1.0013	1.0016	1.0020	1.0032	1.0034	1.0050	1.0051	1.0045	1.0046	1.0060
35.0	1.0002	1.0003	1.0004	1.0009	1.0014	1.0018	1.0021	1.0034	1.0038	1.0053	1.0055	1.0048	1.0049	1.0062